Trade Study and Analysis for a Deployable Drag Device for Launch Vehicle Upper Stage Deorbit

AE8900 MS Special Problems Report
Space Systems Design Lab (SSDL)
Guggenheim School of Aerospace Engineering
Georgia Institute of Technology
Atlanta, GA

Author:
Alexandra C. Long

Advisor:
Dr. David A. Spencer

May 2, 2015

Trade Study and Analysis for a Deployable Drag Device for Launch Vehicle Upper Stage Deorbit

Alexandra C. Long* and David A. Spencer†

Georgia Institute of Technology, Atlanta, GA, 30332-1510, USA

Orbital debris is a growing problem in low Earth orbit; it has crossed a threshold of critical density where the number of debris objects will grow exponentially unless mitigated. Spent launch vehicle upper stages represent a problematic category of orbital debris in highly utilized orbits. They can stay in orbit for well over 100 years if left to deorbit naturally, and they represent a significant fraction of large space debris in low-Earth orbit. It is estimated that removing a few large objects per year will mitigate the exponential growth of debris. To address the debris problem, a trade study was conducted to determine a deployable drag device to accelerate the orbit degradation of upper stages. Following the operation of the upper stage, the drag device will be deployed to decrease the orbit lifetime of the system. The design is targeted toward upper stages launched into orbital altitudes ranging from 650-850 km. Three categories of deployable drag devices are being investigated: drag sails, inflatable aerodynamic decelerators, and electrodynamic tethers. These are compared to the option of using residual propellant in the upper stage to perform a burn to initiate a deorbit trajectory. The device will be mounted to the upper stage using a standardized secondary payload launch interface, such as a CubeSat deployer device or the EELV Secondary Payload Adapter (ESPA). The trade study compared the drag device configurations based on cost, risk, and deorbit time. A maximum deorbit period of 25 years is a performance design requirement. The propulsive option was shown to be the lowest cost option, however the drag device is more mass efficient and has less of an impact to the payload capability of the launch vehicle. A drag sail design is proposed as a baseline design for the device. A stability analysis was conducted to determine the configuration of the device, then the initial baseline design with preliminary component selection and an initial structural analysis were investigated.

Nomenclature

LEO	Low Earth Orbit
$ESPA$	EELV Secondary Payload Adapter
$EELV$	Evolved Expendable Launch Vehicle
$PPOD$	Poly-Picosatellite Orbital Deployer
AHP	Analytical Hierarchy Process
P/L	Payload
ATP	Area-Time Product
$type$	Relative weighting of risk criteria
$2pay$	Risk of adherence to secondary payload requirements
$ndeb$	Risk of creating new debris
$fdep$	Risk of device not fully deploying
$sdep$	Risk of device not staying deployed
$f10$	Solar radio noise flux
$f10b$	162-day average f10
gi	Geomagnetic activity
C_L	Coefficient of Lift

*Graduate Research Assistant, Daniel Guggenheim School of Aerospace Engineering, AIAA Student Member

†Professor of the Practice, Daniel Guggenheim School of Aerospace Engineering, AIAA Member

C_D	Coefficient of Drag
ε	Fraction of molecules reflected specularly
s	Speed ratio of the freestream,
α	Angle of attack, radians
T_r	Temperature of the surface, Kelvin
T_∞	Freestream static temperature, Kelvin
ϕ	Half-angle between sails, radians
γ	Angle between axis of upper stage and axis of device, radians
SRP	Solar Radiation Pressure
ν	Shadow function
P_{rad}	Solar radiation pressure constant, 4.56x10^{-6} N/m^2
β	Angle between sunlight and sail normal, radians
A	Area of sail, m^2
ϵ	Reflectivity
$\mathbf{e}_\odot$	Unit vector from sail surface to the sun in flow frame
$\mathbf{n_i}$	Normal vector for the front of the sail
ρ	Atmospheric density
U_∞	Freestream Velocity
L	Length of sail
w	Width of sail
L/V	Launch Vehicle
CAD	Computer Aided Drafting
B	Billow angle of sail

Subscript

i	Variable number

I. Introduction

Orbital debris is a growing problem in low Earth orbit; it has crossed a threshold of critical density, known as Kessler Syndrome, where the number of debris objects will grow exponentially unless mitigated as a result of objects colliding and creating more debris. When the Cosmos and Iridium satellites crashed in 2009, 2000 trackable objects and on the order of 100,000 untracked objects were added to orbit.[1] It has been shown that removing five large objects from Low Earth Orbit (LEO) per year will mitigate Kessler Syndrome, if started by 2020.[2] There have been many proposed systems for active removal of debris from orbit. A more efficient, and far less costly approach is to accelerate the orbital decay of large space systems through the use of passive drag devices.

Spent launch vehicle upper stages represent a problematic category of orbital debris in highly utilized orbits. They can stay in orbit for well over 100 years if left to deorbit naturally, and they represent a significant fraction of large space debris in low-Earth orbit.[3] This research is focused on accelerating the orbit degradation of launch vehicle upper stages by using a deployable drag device that can be launched as a secondary payload and deployed using a standard deployment system for secondary payloads. Following the operation of the upper stage, the drag device will be deployed to passively decrease the orbit lifetime of the system. It will be stowed in using the size and mounting constraints of current secondary payload standards to enable the use of current architecture on upper stages. This paper discusses three initial steps in the design. The first is the trade study that was conducted to compare the drag device configurations based on cost, risk and deorbit time. The second is the stability analysis conducted to determine the aerostable design. The third is the device design that includes material selection and preliminary analysis.

II. Trade Study

A trade study was conducted to determine the best configuration for this passive deployable drag device. The explanation of the is divided into three parts: the description of the parameters, the explanation of the

analysis and the results of the study.

II.A. Parameters

The trade study involved five main areas: device type, launch vehicle, target orbit altitude, design decay time, and packaging volume. The different options in each category can be seen in the Morphological Matrix in Table 1.

Table 1: Morphological Matrix for drag device trade study

Architecture Decision	Option 1	Option 2	Option 3	Option 4	Option 5	Option 6
Device Type	Drag Sail	Inflatable Balloon	Tether	Propulsive		
Launch Vehicle	Falcon 9	Delta IV	Atlas V			
Target Orbit Altitude	High LEO (850-1000 km)	Mid LEO (700-850 km)	Low LEO (600-700 km)			
Design Decay Time	25 years	15 years	10 years	5 years		
Packaging Volume	3U PPOD	6U PPOD	12U PPOD	27U PPOD	1/2 ESPA	Full ESPA

II.A.1. Device Types

There are four main device types that are considered for orbit debris removal. The first is a drag sail, which is similar in concept to a solar sail. For the initial trade study, it was assumed to be a square planar sail comprised of four booms that support a thin membrane, as seen in Figure 1. Additional hardware includes a deployment motor and electronics to initiate deployment.

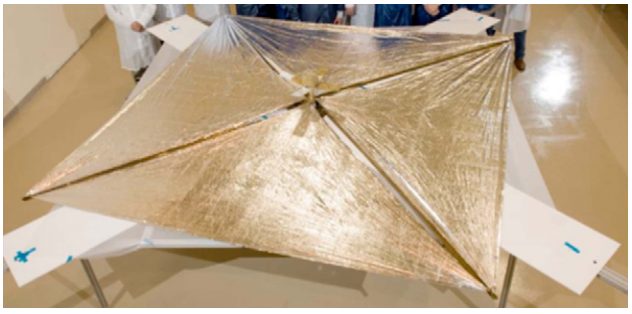

Figure 1: NanoSail-D solar sail, similar design to drag sail in trade study[4]

The second device type is an inflatable balloon. It was assumed to be a thin membrane that is inflated with a gas to form the shape of a sphere,[5] as seen in Figure 2. It was decided not to have the membrane rigidized because collisions with the non-rigidized balloon have a lower risk of creating more debris.[6]

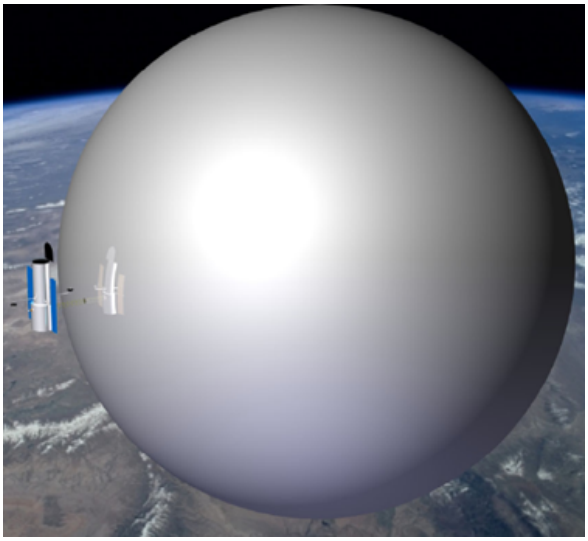

Figure 2: Gossamer Orbit Lowering Device (GOLD), similar to inflatable balloon used in trade study[5]

The third device is an electrodynamic tether. The electrodynamic tether interacts with the Earths magnetic field in such a way that it creates a drag force that decreases deorbit time,[7] as shown in Figure 3.

The fourth approach to deorbit is to utilize the launch vehicle upper stage on-board propellant and guidance system to perform a controlled deorbit. This approach is generally viable, however, allocation of propellant for deorbit reduces the payload mass capability of the launch system. In evaluating propulsive deorbit in this trade study, propellant mass was sized to ensure deorbit within each of the discrete decay times in the morphological matrix.

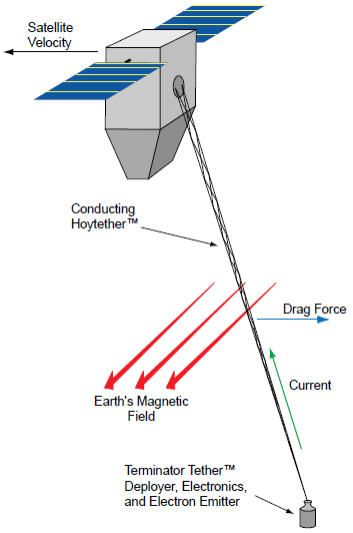

Figure 3: The Terminator Tether, similar to the electrodynamic tether used in the trade study[7]

II.A.2. Launch Vehicles

The launch vehicles were selected for this study (Falcon 9, Delta IV, Atlas V) because they frequently send payloads to highly utilized low-Earth orbits, and they are capable of deploying secondary payloads using standardized deployment devices.

II.A.3. Target Orbit Altitudes

Low Earth Orbit (LEO) is generally defined as altitudes of 600-1000 km. This was divided into three ranges: Low LEO (600-700km), Mid-LEO (700-850 km), and High LEO (850-1000 km). The upper limit of each altitude range for the target orbit altitude was investigated.

II.A.4. Design Decay Time

Across the world, many space organizations are creating guidelines for how long defunct objects can remain in space. Across the board, that limit is 25 years. This analysis was hoping to make deorbit time as small as possible to reduce risk. The times are 25 years, 15 years, 10 years, and 5 years.

II.A.5. Packaging Volume

It was decided to use secondary payload mass and volume requirements consistent with standardized secondary payload deployment systems. Each of the launch vehicles listed in Table 1 are capable of deploying secondary payloads. Therefore, treating the deployment device as a secondary payload does not pose any new design requirements on the launch system.

Six different types of secondary payload packaging were investigated. The first four are different sizes of the Poly-Picosatellite Orbital Deployer (PPOD), which is the original CubeSat launching platform. One unit of a CubeSat, or 1U, has dimensions of 10 cm x 10 cm x 11 cm. A 3U PPOD holds a satellite with three of these in line for dimensions of 10 cm x 10 cm x 34 cm.[8] The 6U PPOD is two 3Us next to each other, and so on.[9] With increasing volume, there is an increasing amount of mass allowed as well. The 3U has a maximum mass of 4 kg, and the 6U has a maximum mass of 12 kg.

The mass and volume requirements of the different packaging can be seen in Table 2. The final two stowing packaging are the Evolved Expendable Launch Vehicle (EELV) Secondary Payload Adapter (ESPA) class payloads. They come in full and half sizes. ESPA payloads have less strict shape requirements than PPODs, but the volume dimensions listed in Table 2 are the general space envelope each payload is given on the launch vehicle.[10]

Table 2: Dimensions for the secondary payload packaging.

Packaging	Dimensions (m)	Volume (m^2)	Mass (kg)
3U PPOD[8]	0.10 x 0.10 x 0.34	0.0034	4
6U PPOD[9]	0.12 x 0.24 x 0.36	0.0104	12
12U PPOD[9]	0.23 x 0.24 x 0.36	0.0199	24
27U PPOD[9]	0.34 x 0.35 x 0.36	0.0428	54
1/2 ESPA[10]	0.50 x 0.50 x 0.60	0.1500	90
Full ESPA[10]	0.61 x 0.71 x 0.91	0.3587	181

II.B. Analysis

There were three main variables that were used in a pareto evaluation: risk, deorbit time, and cost. In order to estimate the pareto variables for each configuration, the drag area and mass were also estimated.

II.B.1. Drag Area

The drag area is one of the most important characteristics of the drag sail and the inflatable for this analysis because it is used to estimate deorbit time, collision risk, and cost. The first step in the analysis was to use historical data to estimate the drag area that could be stowed in the different packaging.

Estimating Drag Sail Drag Area The historical missions used as benchmarks were all square solar sails. NanoSail-D is a mission developed by NASA Marshall Spaceflight Center. It had a deployed area of 10 m^2 and was packaged in a 3U CubeSat.[4] CubeSail is a mission by the University of Surrey to demonstrate solar sailing. It has a deployed area of 25 m^2 and is packaged in a 3U CubeSat.[11] LightSail is another solar sailing demonstration mission sponsored by The Planetary Society. It has a deployed area of 32 m^2 and was packaged in a 3U CubeSat.[12] Sunjammer was a cancelled mission by LGarde, Inc. to demonstrate a mission capable solar sail. It had a deployed area of 1200 m^2 and was packaged in a full ESPA.[13]

In order to compare the deployed area to the packaging volume, the packing coefficient was calculated by dividing the deployed area by the stowed volume. The values ranged from 5,000 m^{-1} for NanoSail-D to 21,000 m^{-1} for Sunjammer. The estimated deployed areas for each packaging were estimated using a packing coefficient of 16,000 m^{-1}. The values can be seen in Table 3. It was assumed that 70% of the volume would be taken up by the sail and the remaining 30% by other subsystems. Since the drag sail is assumed to be flat, there is no guarantee that it will trim to a maximum drag attitude perpendicular to the flow. To account for this, the drag sail normal was assumed to be oriented 60°away from the flow, so the drag area is estimated as the deployed area multiplied by sin(30°). These values are also shown in Table 3.

Table 3: Calculated deployed and drag areas for the drag sail and inflatable that can be packaged in each packaging size.

Packaging	Drag Sail Deployed Area (m^2)	Drag Sail Drag Area (m^2)	Inflatable Drag Area (m^2)
3U PPOD	38	19	50
6U PPOD	116	58	151
12U PPOD	223	111	289
27U PPOD	479	240	621
1/2 ESPA	1680	840	2176
Full ESPA	4017	2009	4882

Estimating Inflatable Balloon Drag Area The historical data used was the Gossamer Orbit Lowering Device designed by the Global Aerospace Corporation. It is a 37 m diameter sphere with a mass of 39 kg packaged in a volume slightly larger than a 27U PPOD.[5]

It was assumed that the inflatable balloon would package similar to parachutes by using a constant packing density. The packing density is the amount of parachute mass that can be packaged into 1 cubic meter of volume[14] . The mass was divided by the packaging volume to get the packing density. The estimated packing density used was 746 kg/m^3. To estimate the drag areas, the packing density was multiplied by the stowing volume to get the mass, which was in turned divided by the areal density of 0.009 kg/m^2 to get the surface area. The drag area is the area of the circular cross section of the deployed sphere. The drag areas are shown in Table 3.

II.B.2. Mass

For each packaging, the maximum mass allowed was based upon the constraints of the secondary payload deployment device. For the propulsion option, it was necessary to use the rocket equation to calculate the mass of propellant needed to perform a deorbit burn to ensure specified deorbit times. This mass was then used to calculate the cost of this option for each launch vehicle based upon their price per kilogram of payload mass that can be delivered to the specified orbit.

II.B.3. Risk

Risk is an important parameter for decision making, but it is difficult to quantify. This analysis was divided into two halves that were recombined at the end to have a quantitative value for each option. The first half

used the Analytical Hierarchy Process (AHP) to conduct a series of piecewise comparisons. The second half was calculating the area time product.

Analytical Hierarchy Process for Risk Each device type was evaluated based on four different criteria: how well the device adheres to secondary payload requirements, the risk of creating new debris, the risk it will not fully deploy, and the risk that it will not stay deployed. Table 4 shows the first step which is to create a matrix of comparing the criteria to each other in terms of importance. Then, for each criterion, a matrix is created to compare each device to each other. These can be seen in Tables 5, 6, 7 and 8.

These matrices were created by assigning a value to one option over another. The value in each cell is the value of the option on the left divided by the value of the option on the top. For example, in Table 4, adhering to secondary payload requirements is twice as important as creating new debris, therefore the second cell in the first row is 2, and the first cell in the second row is 0.5.

The next step is calculating the normalized vectors of each matrix by squaring the matrix, calculating the row sum, and then normalizing that vector. This is repeated until the vector does not changed between iterations. These will be used at the end of the risk analysis to combine the comparisons into a single numerical value.

The comparison numbers in Table 4 were determined by importance. The secondary payload requirements were determined to be more important than creating new debris because adherence to secondary payload requirements determines the ease in which the device is integrated into the launch vehicle with the other payloads. It is also more important than fully deploying and staying deployed because increasing integration complexity increases cost. Creating new debris is more important than fully deploying and staying deployed because the purpose of this device is to decrease debris, not create more. Staying deployed and fully deploying are equal because they both determine how effective the device is while in orbit.

Table 4: Relative weighting of risk criteria (type)

	2nd P/L Reqts	New Debris	Fully Deploy	Stay Deployed
2nd P/L Reqts	1	2	3	3
New Debris	0.5	1	2	2
Fully Deploy	0.3333	0.5	1	1
Stay Deployed	0.3333	0.5	1	1

Table 5 shows the comparison for adherence to secondary payload requirements. Propulsion is the least risky because it does not require any modifications to the launch vehicle itself. The inflatable is riskier than propulsion because its inflation mechanism will most likely require a waiver from the launch vehicle provider, and riskier than the drag sail because the drag sail will just need to prove proper inhibits are in place. The tether is equal in risk as the drag sail because it will also only need proper inhibits. Both the drag sail and tether are riskier than propulsion.

Table 5: Adherence to secondary payload requirements piecewise comparison of the devices (2pay)

	Drag Sail	Inflatable	Tether	Propulsion
Drag Sail	1	0.5	1	2
Inflatable	2	1	2	3
Tether	1	0.5	1	2
Propulsion	0.5	0.3333	0.5	1

Table 6 shows the risk the device will create new debris. The drag sail is riskier than the inflatable because the drag sail has rigid booms supporting the flexible film and the inflatable is entirely a flexible film. If an objects hits the film, it will most likely not fracture into smaller pieces, but if it hits the rigid boom it will fracture. The propulsion is riskier than the drag sail and inflatable because the upper stage will be drifting

after the burn, and the entire upper stage is rigid. The tether is the riskiest because it is very long and would cross the path of many satellites, and not all will have the ability to avoid it. It will also be hard to detect in order to avoid.

Table 6: Create new debris piecewise comparison of the devices (ndeb)

	Drag Sail	Inflatable	Tether	Propulsion
Drag Sail	1	2	0.3333	0.6667
Inflatable	0.5	1	0.25	0.5
Tether	3	4	1	2
Propulsion	1.5	2	0.5	1

Table 7 shows the risk the device will not fully deploy. Propulsion is the least risky because the engines will only need to be restarted. Next is the inflatable, which is riskier than propulsion because the deployment is based on the effectiveness of the inflation mechanism and folding scheme. The drag sail is riskier than the inflatable because it requires unfolding the booms and the sail, which is complicated and precise. The tether is the riskiest because it has a much longer single length to deploy, and tethers in the past have often gotten tangled during deployment.

Table 7: Risk it will not fully deploy piecewise comparison of the devices (fdep)

	Drag Sail	Inflatable	Tether	Propulsion
Drag Sail	1	2	0.3333	3
Inflatable	0.5	1	0.6667	2
Tether	3	6	1	9
Propulsion	0.3333	0.5	0.1111	1

Table 8 shows the risk that the device will not stay deployed. This is trivial for the propulsion option because the burn would be a discrete event. The drag sail also is low risk because once it is deployed, the booms will lock in place ensuring it will stay deployed, and the sail film can be designed to minimize damage from debris. The inflatable is riskier than the drag sail because if it is struck by debris, no matter how small the hole, the inflation gas will leak, preventing it from staying deployed. The tether is the riskiest because it could be tangled or cut as a result of collisions with debris.

Table 8: Risk it will not stay deployed for the duration of deorbit piecewise comparison of the devices (sdep)

	Drag Sail	Inflatable	Tether	Propulsion
Drag Sail	1	0.5	0.3333	1
Inflatable	2	1	0.6667	2
Tether	3	1.5	1	3
Propulsion	1	0.5	0.3333	1

Area-Time Product Area-Time Product (ATP) is not a measure of the actual risk of creating new debris, but it is proportional to the risk and easier to calculate. Nock et. al[6] describe how to calculate this using the collision cross sectional area instead of the drag area, as shown in Figure 4. The collision area assumes a nominal debris size of 2 m and adds a 1 m buffer to the outside of the object to create the collision area.[6]

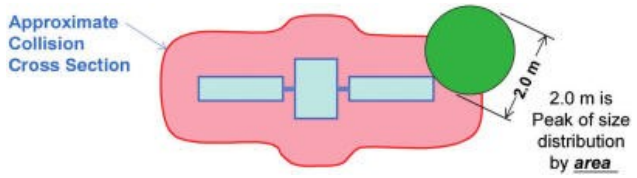

Figure 4: Collision area used in the area-time product[6]

In order to combine this with the eigenvalues from AHP, the ATP values must be normalized by the range of values using Equation (1).

$$|ATP_i| = \frac{ATP_i - ATP_{min}}{ATP_{max} - ATP_{min}} \tag{1}$$

The AHP eigenvalues were then combined with the normalized ATP for each option by Equation (2).

$$Risk = 2pay * type + fdep * type + sdep * type + ndeb * |ATP_i| \tag{2}$$

This gives a single value of risk for each option that is between zero and one, as shown in the pareto plots in Section II.C.

Justification Against Tethers According to Hoyt and Forward, an electrodynamic tether needs to be about 7.5 km long to deorbit a 1500 kg satellite. The interaction with the atmosphere makes tethers ineffective at inclinations above 75°.[7] These requirements lead to the conclusion that tethers are not appropriate for this scale since most of the upper stages investigated are larger than 1500 kg, i.e. the Falcon 9 upper stage is 4900 kg. The tether would pose a risk to other satellites in a similar orbit. The analysis also showed it to be the riskiest of the options. Based upon this, the electrodynamic tether was not considered as a candidate in the pareto evaluation.

II.B.4. Deorbit time

The deorbit time was calculated using the NASA Debris Assessment Software 2.0.2 (DAS). The Science and Engineering utility can calculate the orbit lifetime of an object given certain parameters.

The start year is needed to determine the atmospheric properties during the deorbit period because of the variations of the 11 year solar cycle. The last solar maximum was in 2013. The chosen start year was mid-2015 roughly halfway between solar maximum and solar minimum. This is assumed to be a worst case deorbit time.

The initial orbit for each system is assumed to be circular. Initially, the highest of the three target orbit altitude ranges from Table 1 were evaluated (700 km, 850 km, and 1000 km).

The inclinations in LEO that have the highest concentration of debris are 71-74°, 81-83° and Sun-sync.[1] An inclination of 71° was chosen for the design as the worst case scenario for the most populated orbits since it has the longest decay time. The Right Ascension of the Ascending Node and the Argument of Perigee were set to 0° to simplify the analysis.

The final parameter is the area-to-mass ratio of the system. It was assumed that the mass was only from the upper stage since our mass estimate for the deorbit devices are only 1-3% of the upper stage mass. The area was assumed to be the drag area of the device because it is much larger than the drag area produced by the upper stage.

One thing to note about this analysis tool is that it stops propagating the orbits at 100 years. In the following results, if there is a deorbit time of 100 years, that means at least 100 years.

II.B.5. Cost

The cost was estimated separately for the propulsion options and for the drag sail and inflatable options. Both used historical data for estimates.

Propulsion Cost Estimation The propulsion option was estimated using the price per kg to launch into LEO for each launch vehicle. This was calculated by dividing the cost per launch by the number of kg of payload that could be delivered to LEO. This can be seen in Table 9[a].

Table 9: Cost estimation of propulsion option for each launch vehicle.

	Launch Cost	Mass to LEO (kg)	Price per kg
Falcon 9[15]	$61,200,000	13,150	$4,600
Delta IV[16]	$80,000,000	12,900	$6,200
Atlas V[17]	$100,000,000	9,800	$10,200

Drag Sail and Inflatable Cost Estimation The cost estimation for the devices was based on the cost of LightSail and Sunjammer. The LightSail mission cost is estimated as $2 million while the Sunjammer cost is estimated as $27 million.[18] Both are technology demonstration missions so the cost includes more than the sail subsystem and deployment hardware, as well as the cost decreases once more than one is produced. LightSail is mostly a solar sail, so the cost of the sail subsystem for the first device was assumed to be 40% of the total mission cost, then 55% of that would be the recurring cost of one device, $440,000. Sunjammer is a more complicated system. The mission is composed of two spacecraft: the carrier to help it escape Earth orbit and the sailcraft which is the solar sail plus the electronics needed to make the sail work. The sailcraft is only 1/3 of the volume of the total mission[b], and since it has scientific instruments it was assumed that the cost of the first device was 15% of the total mission cost. With 55% of that cost is recurring, the cost of one device was assumed to be $2,200,000.

It was decided that the cost would scale according to the drag area with a logarithmic trendline. The plotted values are shown in Figure 5. The drag sail costs were extrapolated directly by using the equation of the trendline and the inflatable cost was 2 times the equation of the trendline since the surface area of the inflatable device is at least twice that of the drag sail.

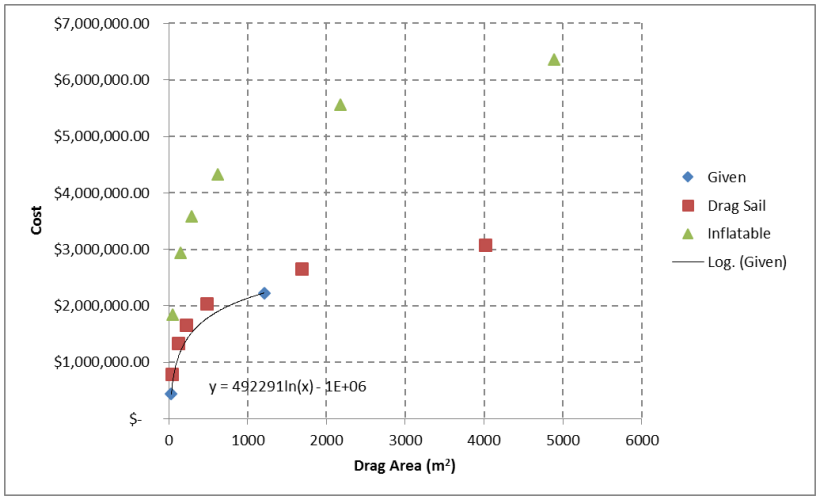

Figure 5: Plot used to estimate the cost based on drag area.

[a]Atlas V data also from personal communications on August 21, 2014 with C. M. Bell in the Communications Department of the United Launch Alliance

[b]Information from personal communications on January 30, 2014 with O. Eldad, graduate student at the University of Texas at Austin

II.C. Results

It was quickly found that an altitude of 850 km is an appropriate choice for a baseline design because it may easily be scaled down for lower altitudes, and the drag force at 1000 km is too small for reliable deorbit based on drag. The different device options were compared for deorbiting from an altitude of 850 km.

The pareto plots that were created are shown in Figures 6, 7, and 8. The grouping for risk and cost are due to the estimation procedure that was used. In all three plots, the propulsive deorbit approach appears to be favored. However, this approach would result in a significant reduction in payload delivery capability for the launch system. This is the primary motivation for flying a low-mass deployable drag device. The goal of this research is to create a fully contained passive drag device system that would only need a single command to initiate deployment. It would require the least amount of work on the launch vehicle providers part to meet the deorbit guideline of 25 years.

With that in mind, it was decided not to choose a configuration that tailored to a specific launch vehicle, but one that would deorbit all three upper stages investigated within the desired 25 years. The different launch vehicles with the same size device can be seen in the plots at three points close together. The chosen "family" is circled in each plot.

In Figure 6, these "families" are lines of positive slope because the larger launch vehicles have longer deorbit times which also is accounted for in the risk. The inflatable is higher risk than the drag sail for adherence to secondary payload requirements and staying deployed. It would require either a chemical reaction or pressure vessel to inflate, which in turn requires a waiver from the launch vehicle provider. Since the inflatable is not rigidized, it could be impacted by debris, causing holes that would prevent it from staying inflated.

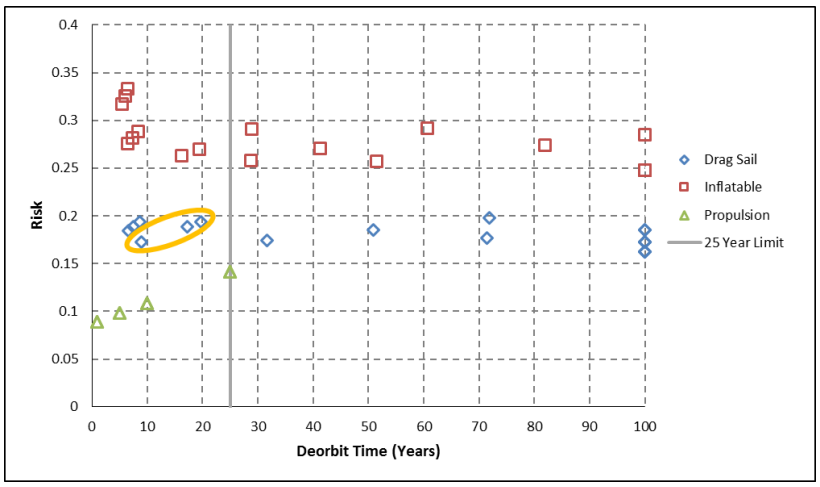

Figure 6: Pareto plot comparing the risk and deorbit time of the various configurations.

In Figure 7, the "families" are horizontal lines because the cost was determined for each size device. It can be seen that the best option where all three points in the "family" falls within the 25 year limit is the second largest drag sail, which is stowed in 1/2 ESPA packaging.

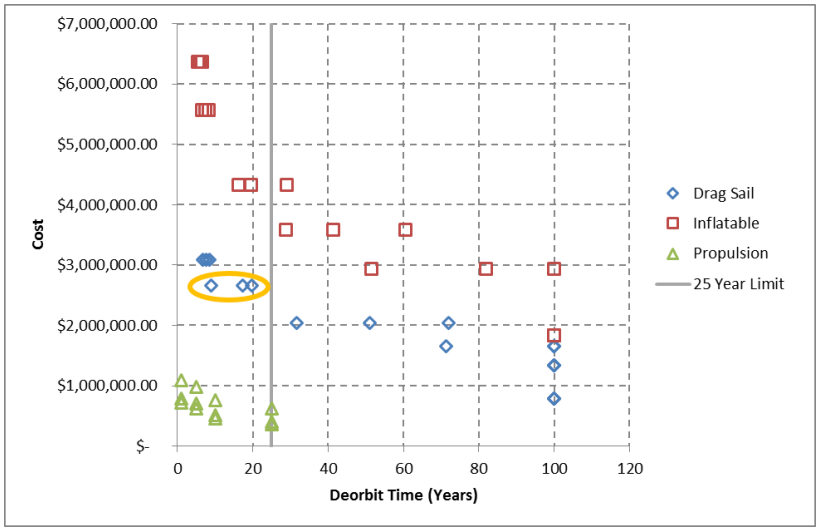

Figure 7: Pareto plot comparing the cost and deorbit time of the various configurations.

In Figure 8, they are vertical lines because the cost is now on the horizontal axis. This is harder to determine the best option because the more ideal points, those with lower risk and lower cost, correspond to the longest deployment times.

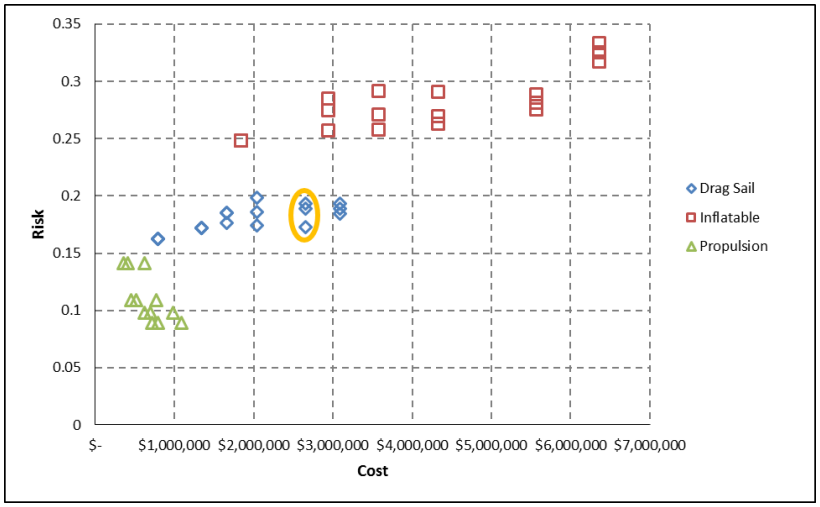

Figure 8: Pareto plot comparing the risk and cost of the various configurations

Therefore, the chosen option is the drag sail in the 1/2 ESPA pacakging. The choice of a drag sail brought up concerns about how to ensure it will create the maximum drag area without active control. In the next section, it will be discussed how the flat square sail design was modified so that if it is disturbed from its nominal maximum drag attitude, it will automatically create restoring moments.

III. Stability Analysis

An aerostable design allows the sail area to be reduced from the 60° off normal angle assumed for the flat drag sail in the trade study. A number of different options were investigated. Then the aerodynamic forces and moments were calculated to verify the stability.

III.A. Design Concepts

The two initial ideas for passively controlling the sail were: using gravity gradient to ensure the upper stage is pointed toward Earth with the sail pointed at the flow, and using a square pyramid shaped sail, as seen in Figure 9. The square pyramid design was difficult to incoporate with the upper stage, so the two ideas were combined to create a hinged plate design, as seen in Figure 10.

This design required less packaging volume than the square pyramid and does not solely rely on gravity gradient for stability. Figure 10 also shows the disturbance torques on this design calculated for all altitudes in the device's lifetime. The solar radiation pressures were calculated with the assumption that the front of the sail has a reflective coating and the back has an absorptive coating to aid deorbit, because solar radiation pressure is the strongest force at the beginning of the deorbit phase. It should also be noted that the gravity gradient is only slightly larger than the atmospheric drag torque for the beginning of the lifetime. Two conclusions were drawn from this: gravity gradient was too weak to rely upon for stabilizing the device, and there should be a smaller moment arm between the center of mass of the system and the center of pressure of the sail.

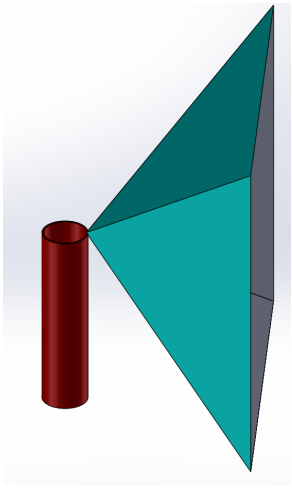

Figure 9: Square pyramid aerostable design with upper stage.

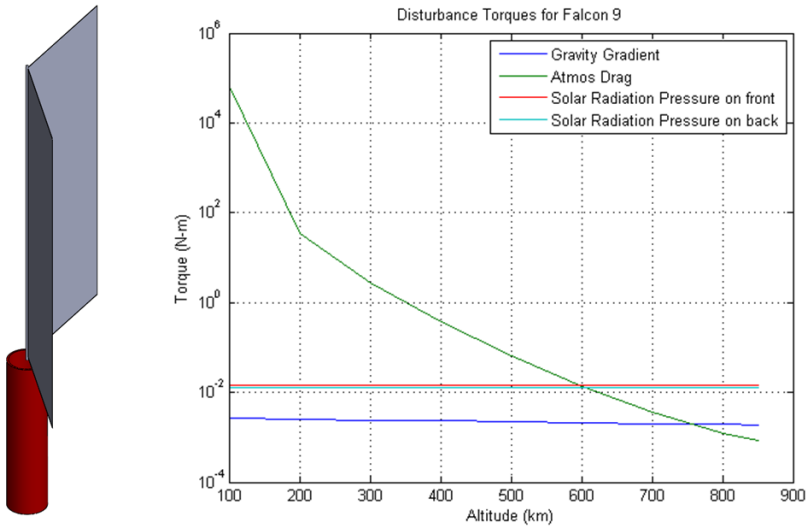

Figure 10: Single hinged plated design with upper stage (left) and the disturbance torques at various altitudes (right)

The solution was to split the device into two smaller devices coming from either end of the upper stage, and

angle them away from the center axis, as seen in Figure 11. The stability was analyzed at multiple altitudes and angles of attack. It was shown that if there is a perturbation from the nominal position of facing toward the flow, the shape of the system creates a restoring torque that moves it back to the nominal position. The double hinged plate design changes the secondary payload packaging from one 1/2 ESPA to two 27U PPODs.

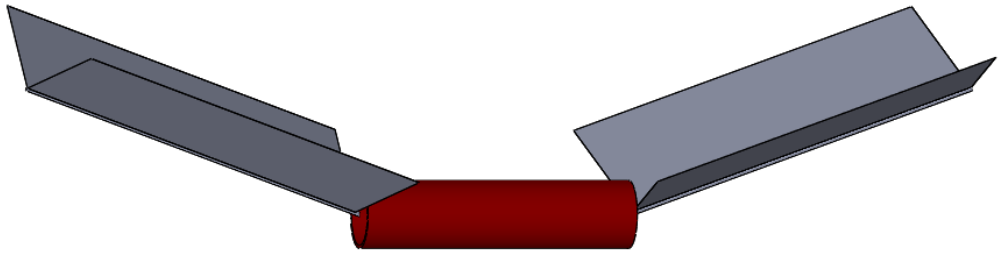

Figure 11: Double hinged plate design

III.B. Analysis

Only two disturbance torques were taken into account for the stability of the double hinged plate design: aerodynamic pressure and solar radiation pressure (SRP). The gravity gradient was not considered because it is an order of magnitude smaller than the two mentioned for most of the deorbit. All other disturbances that effect orbital parameters would average out over the deorbit period.

III.B.1. Atmospheric Model

In order to calculate both the aerodynamic pressure and SRP, it is important to know the density and freestream static temperature of the atmosphere at the desired altitudes. This is very difficult to predict. This research used a program based on the Jacchia 1970 atmospheric model[19] that was modified to include the U.S. 1976 Standard Atmosphere[20] that was written by Mike Hikey and modified by Joseph White at NASA Marshall Space Flight Center. This program requires a number inputs, most of which are easily found (like the date, time, altitude, etc) but others that are less obvious (solar radio noise flux (f10), 162-day average f10 (f10b), and the geomagnetic activity index (gi)). Every month, NASA Marshall Space Flight Center publishes a report about the past, current, and predicted future values of solar activity.[21] The values were found in Table 3 of the April 2015 report.

III.B.2. Aerodynamic Stability

It was assumed that the device is in collisionless, or free molecular, flow. The device-upper stage system was modeled as a cylinder with two plates at various angles coming off either end. The two devices are symmetrical in terms of size and angles with the upper stage. The coefficients of drag and lift were calculated using equations for free-molecule aerodynamics of a flat plate then summed together. The equations can be seen in Equation (3) and Equation (4).[22] These equations came from integrating the shear stress and surface pressure over a complete plate.

$$C_L = \frac{4\varepsilon}{\pi^{\frac{1}{2}} s} \sin\alpha \cos\alpha \exp\left(-s^2 \sin^2\alpha\right) + \frac{\cos\alpha}{s^2}\{1 + \varepsilon(1 + 4s^2 \sin^2\alpha)\} \times \operatorname{erf}(s\sin\alpha) + \frac{(1-\varepsilon)}{s}\pi^{\frac{1}{2}} \sin\alpha\cos\alpha\left(\frac{T_r}{T_\infty}\right)^{\frac{1}{2}} \tag{3}$$

$$C_D = 2\frac{\{1-\varepsilon\cos(2\alpha)\}}{\pi^{\frac{1}{2}}s}\exp\left(-s^2\sin^2\alpha\right) + \frac{\sin\alpha}{s^2}[1+2s^2+\varepsilon\{1-2s^2\cos(2\alpha)\}]\,\mathrm{erf}(s\sin\alpha) + \frac{(1-\varepsilon)}{s}\pi^{\frac{1}{2}}\sin^2\alpha\left(\frac{T_r}{T_\infty}\right)^{\frac{1}{2}} \quad (4)$$

The Bird book[22] provides two graphs of the lift and drag of a flat plate at discrete values of ε, which is a material property of the plate. The first graph is for the lift of a flat plate and can be seen in Figure 12a. Figure 12b is the version created as validation for one plate offset from the center of mass. It can be seen that they agree except they are mirrored vertically; this is due to a difference in the definition of angle of attack. The second graph is for the lift-drag ratio of a flat plate. The figure from Bird and the generated graph can be seen in Figures 13a and 13b. In order to use these equations, it must be verified that the free molecular flow assumption is valid. This is done by calculating the Knudsen number, the ratio between the mean free path and the characteristic length. The Knudsen number for this situation is about 70,000, which is much greater than 1000 verifying that this device is operating in free molecular flow.[22]

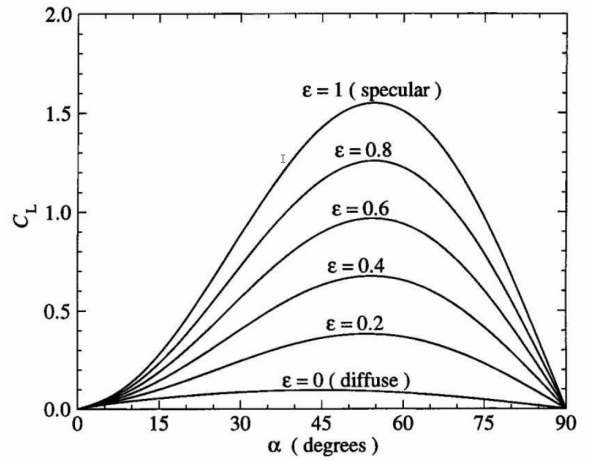

(a) From Molecular Gas Dynamics Figure 7.13[22]

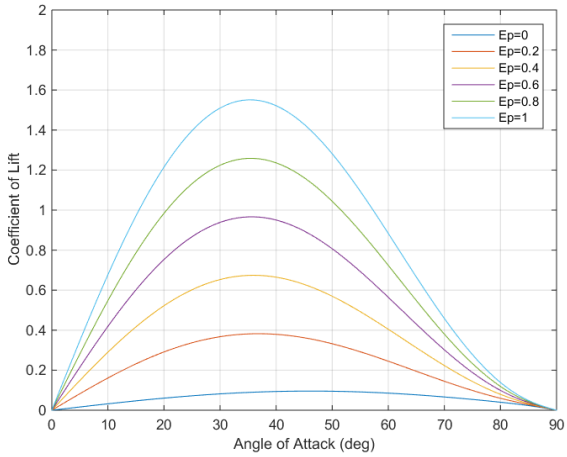

(b) Created using above equations

Figure 12: Lift of a flat plate at s=10 and $T_r = T_\infty$

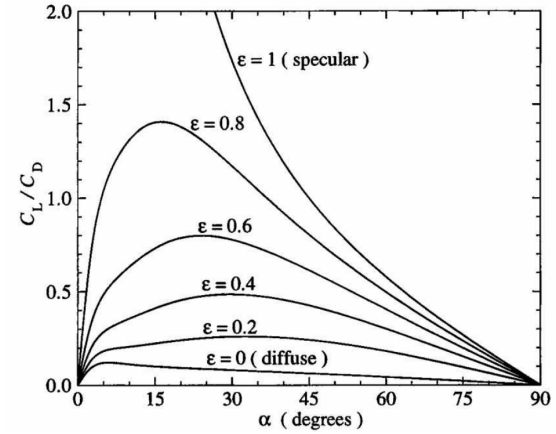

(a) From Molecular Gas Dynamics Figure 7.14[22]

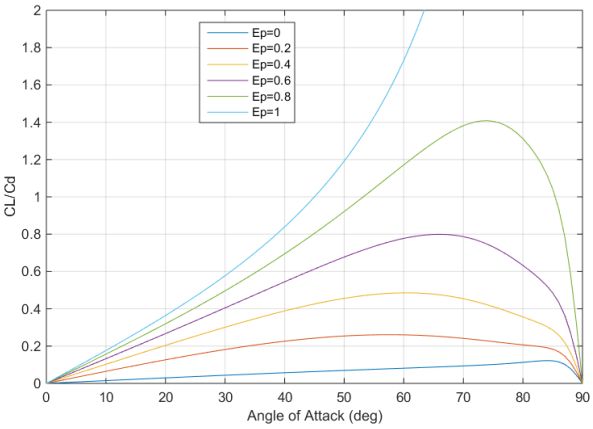

(b) Created using above equations

Figure 13: Lift-drag ratio of a flat plate at s=10 and $T_r = T_\infty$

The next step was taking these equations and applying them to each of the four plates that have different offsets from the center of mass and angles to the flow. The first coordinate system that was defined is the body fixed coordinate system shown in Figure 14a. The origin was set at the center of mass of the system.

The definition of stability is its ability to restore itself back to the nominal position, defined as zero angle of attack (α) shown in Figure 14b. After defining these coordinate systems, Equation (3) and Equation (4) were applied over a range of angles of attack and the results are shown in Figure 15a as the thin solid lines. Stability was assessed by analyzing the moment coefficients in the x, y and z directions over a range of angles of attack by multiplying the radius from the center of mass of the system to the center of mass of each plate perpendicular to each force coefficient. Basically, M=r x F, but resolved by scalar components because the force coefficients are scalars. To keep the moments calculated in coefficient form, the magnitudes of each radius was divided by a reference radius that was half of the length of the upper stage added to half the length of the plate. Figure 15b shows these with the solid lines. It can be seen that the system is stable because the x and z direction moments are zero, while the y moment becomes more negative as the angle of attack grows to 40°. This means that if the device is disturbed up to 40°, a negative moment will be created to counteract the disturbance and reduce the angle of attack. It is rare that a disturbance will be so great as to instantaneously make the angle of attack larger than 40°.

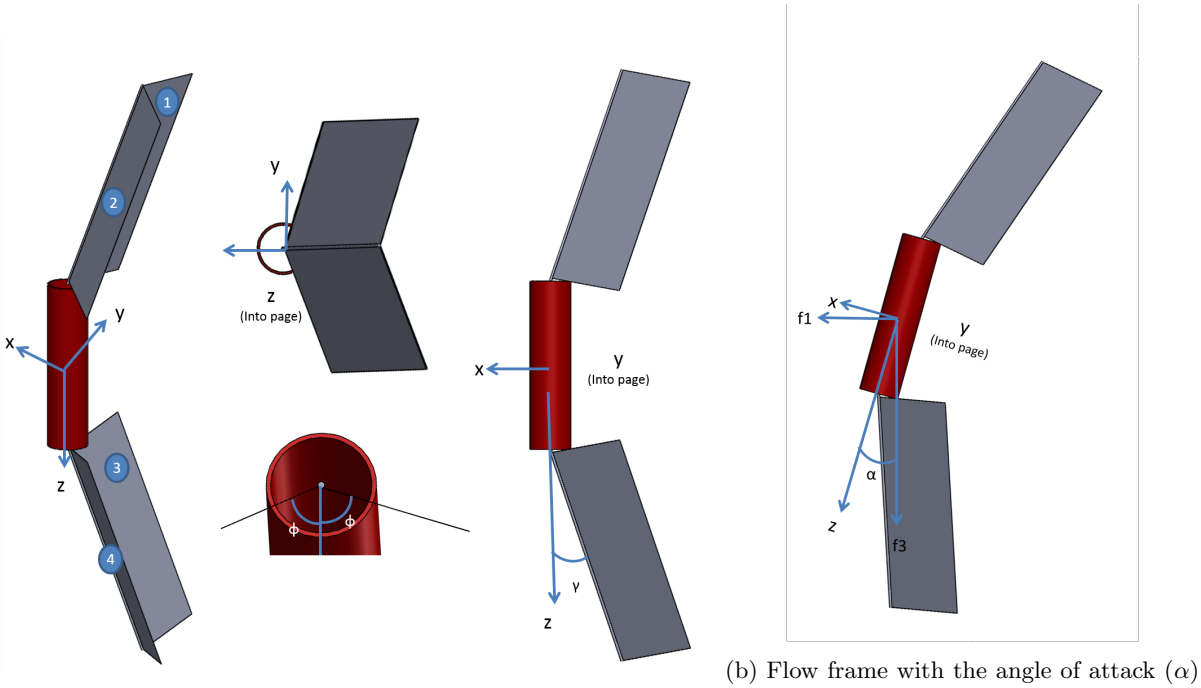

(a) Body fixed with design angles defined

(b) Flow frame with the angle of attack (α) defined

Figure 14: Coordinate system definitions for system

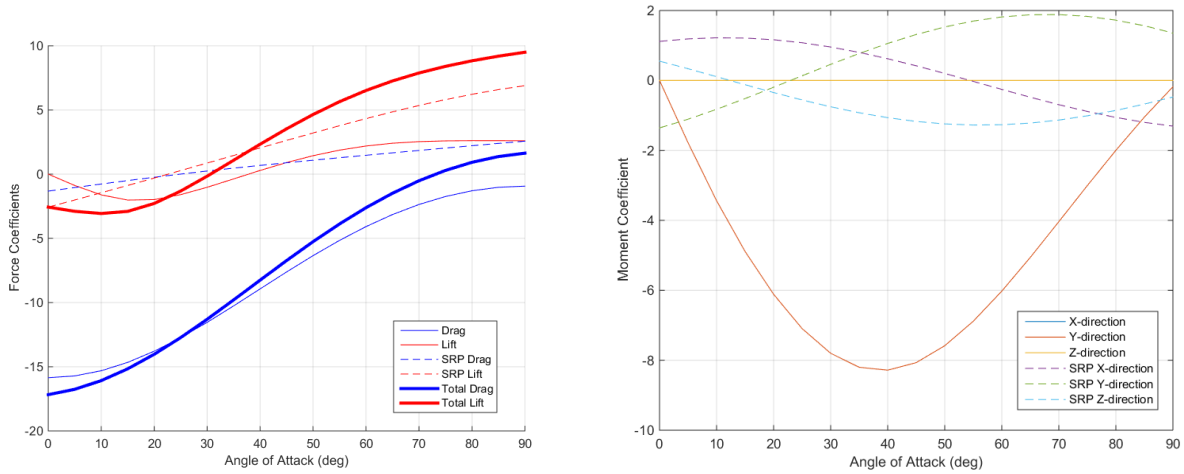

(a) Force Coefficients

(b) Moment Coefficients

Figure 15: Coefficients for double hinged plate for both aerodynamic forces and SRP

III.B.3. Solar Radiation Pressure

The solar radiation pressure was important to calculate because the design orbit starts at 850 km, where solar radiation pressure is greater than atmospheric drag as seen in Figure 16. In order to determine the stability, rough calculations were conducted to determine the SRP at 850 km when the system was in full sun, facing the sun. Equation (5) shows the detailed, simplified model used for each plate, then they were combined with a vector sum.[23] This calculates the true force value and not the coefficient calculated for the aerodynamic forces. To convert them to coefficients, they were divided by the dynamic pressure shown in Equation (6).[22] The moments were created the same as for the aerodynamic forces. These are shown in Figure 15a and Figure 15b as the dashed lines, and it can be seen that the stability is not greatly affected.

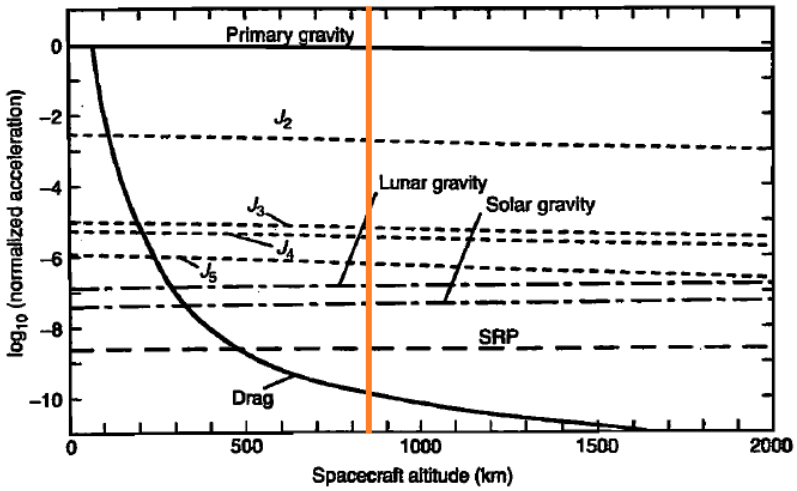

Figure 16: Comparisons of the disturbing acceleration for the main sources of perturbation in the restricted three-body problem.[24]

$$F_i = -\nu P_{rad} \cos\beta_i A_i[(1-\epsilon_i)\mathbf{e}_\odot + 2\epsilon_i \cos\beta_i \mathbf{n_i}] \tag{5}$$

$$q = 1/2\rho U_\infty^2 \tag{6}$$

IV. Device Design

Once a configuration was chosen, the initial design phase was initiated. The first step was defining the high level requirements to clearly state the objectives of the system. Then, a literature review was conducted to determine the different types of booms and sail materials that have been developed for similar systems. This lead to initial component selection, then a preliminary analysis of the baseline design.

IV.A. Requirements

The requirements clearly state the purpose and direction, as well as the design constraints of the system. They start with the Mission Statement, then lower levels were derived from the higher levels. The Mission Statement and the derived Mission Objective are shown below.

Mission Statement: *The deployable drag device shall accelerate the orbital decay rate of launch vehicle upper stages, allowing deorbit to occur within 25 years after launch. The device shall be mounted as a secondary payload on launch vehicle upper stages.*

Mission Objective: *The deice shall deorbit launch vehicle upper stages for the Falcon 9, Atlas V, and Delta IV launch vehicles within 25 years from an initial orbit altitude of 850 km or less.*

Below those two, there are currently four more levels of requirements, some of which have multiple divisions on the same level. The hierarchy is shown in Figure 17. See Table 12 in Appendix A for a complete list of the specific requirements.

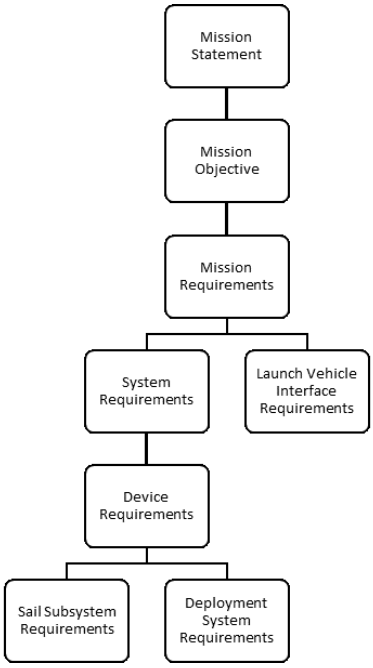

Figure 17: Flow down of requirements by grouping

IV.B. Boom Selection

The stability analysis determined that the long axis is 22 m long, and each panel would be 9 m wide. It was determined that for simplicity and to minimize mass, all of the support structure would be strain energy deployed. While some of these type of booms still need some control during deployment, it is less than those that require a motor to force the deployment. Various deployable booms and trusses were discussed by Banik[25] and Murphey.[26] The trusses are more structurally efficient, but often are more complex to construct.

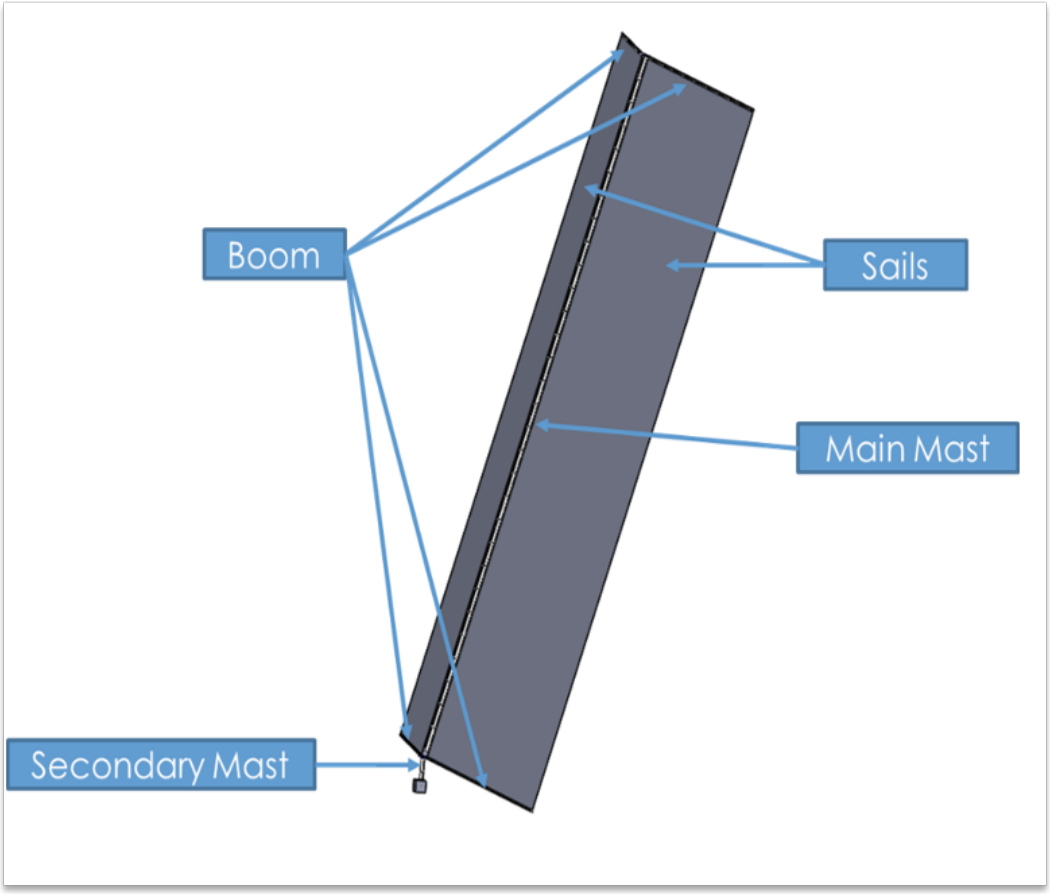

Figure 18: Initial Computer Aided Drafting (CAD) model of design with component terminology labeled.

During boom selection, it was determined that the supports for the long axis need to be a lot stronger because of the much longer length. It was decided to call that the mast, and the supports for the width of the panels would be called booms. This terminology is shown in Figure 18. The main mast was limited to a truss design because of its length, even though they are complex and more expensive. The best option is a coilable boom from ATK, as seen in Figure 19. This design has continuous longerons, the component that lies along the length of the mast, made of graphite that are elastically coiled when the boom is retracted.[26] It is stowed into a cylinder less than 0.7% of deployed length and very mass efficient.[27] Figure 18 mentions a secondary mast, this is a shorter mast, probably about 1 m or so, that will lift the entire stowed device assembly of main mast, booms, and sails out of the packaging that contained it during launch and away from the upper stage. This will allow the device to be angled backward without interfering with the upper stage. It was decided that it will be a shorter version of the mast chosen for the main mast.

The booms, on the other hand,are short enough to take advantage of the heritage from small satellite solar sail designs, like LightSail[12] and NanoSail-D.[4] They used a boom part of the collapsible tube class that is generally lower in structural efficiency, but packs to a smaller volume and is simpler to construct. The best known booms of this class are the Storable Tubular Extendible Member (STEM), the Collapsible Tube Member (CTM) (or Lenticular), and the Triangular Rollable And Collapsible (TRAC) mast. As their name implies, they all can be flattened then rolled around a central hub to be stowed, then they deploy using strain energy as they recover their deployed cross section.[25] The TRAC mast was chosen for the booms because of its large cross section inertia compared to the stowed height. The TRACv4 was chosen from the different variations because of it is strong with a smaller minimum wrap diameter for stowing purposes. The initial version was stainless steel, but the composite versions are stronger.[28] Figure 20 shows the dimensions of the TRACv4 boom baselined for this design.

Figure 19: ATK Coilable Mast, seen partially and fully deployed[27]

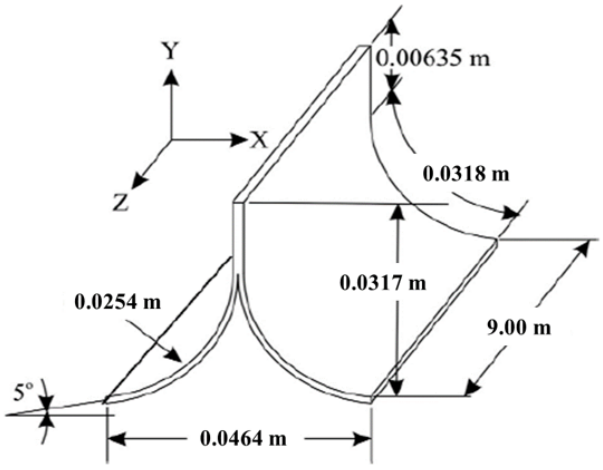

Figure 20: Dimensions of TRACv4 booms[28]

IV.C. Sail Selection

Previous sails have been made from Kapton, Mylar, or a proprietary material produced by SRS Technologies called CP1, which is the thinnest.[29] It has been shown that the chosen membrane material and coating can affect how the sail deploys based on the folds of the sail sticking together too much or not enough.[30] Testing or modeling is required to select a baseline sail material.

The pattern for folding and stowing the sail was investigated and narrowed down to three options: z-folded

then rolled around a hub,[31] z-folded in two directions,[12] or Miura-Ori folding.[32] The first two options are exactly how they sound, Figure 21a shows a diagram on how to fold the Frog Legs pattern that uses z-folding. The difference is that these options would fold the ends so it would be pulled from one direction to deploy, not two.[33] The Miura-Ori pattern can be deployed in two dimensions at the same time by only pulling on one point.[34] It can be seen in Figure 21b. This choice is highly coupled with the deployment procedure, discussed below.

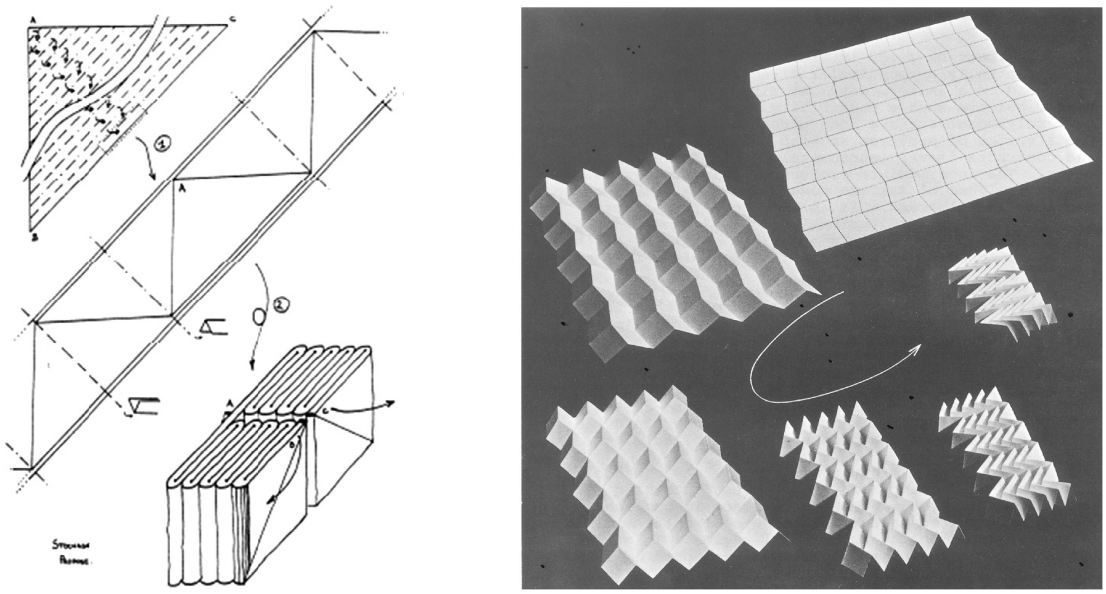

(a) Frog Legs sail folding concept that utilizes z-folding[33]

(b) Miura-Ori folding scheme[34]

Figure 21: Diagrams of different folding scheme options

The first step in any deployment procedure will be deploying the secondary mast to lift the assembly out of the PPOD-like container. After that, there are four possible options detailed in Table 10. The first two options deploy the sail with the mast and booms, and would most likely utilize one of the z-folded schemes. The second two options have the booms and mast fully deploy then a system of pulleys and lanyards would deploy the sail, most likely using a Miura-Ori folding scheme. Once again testing or modeling is required to select the sail deployment procedure baseline.

Table 10: Deployment Procedure Options

Option 1	Option 2	Option 3	Option 4
1. Long mast and sail length deploys 2. Booms and sail width deploys	1. Booms and sail width deploys 2. Long mast and sail length deploys	1. Long mast deploys 2. Booms deploys 3. Sail deploys	1. Booms deploys 2. Long mast deploys 3. Sail deploys

IV.D. Mounting

The device is packaged in a 27U PPOD sized box that has dimensions of 34 x 35 x 36 cm.[9] The secondary and main masts are stowed in clyinders, and the booms are wrapped around a central hub. The base of the secondary mast containment cylinder will be mounted to the bottom of the box. On top of the boom is mounted an angled piece to create the 15° angled back from the central axis. Mounted on top of that is the hub with the two bottom booms. The booms are connected around the hub in such a way that when they are deployed, they create the 160° angle between them. On top of that is the main mast, and at the end of the main mast is the top boom hub. Figure 22a shows how the stowed components fit into the box and Figure 22b shows a close up on the deployed configuration. Figure 22a does not show the sails because it has not yet been determined how they will be stowed. The outside corners of the sails will be connected

to the ends of the booms, and the inside corners will be connected to either the boom hubs or main mast. The exact method of connection needs to be defined.

(a) Stowed components

(b) Close up of bottom of deployed design

Figure 22: CAD models of current design

IV.E. Initial Structural Analysis

The main performance requirement for the strength of the system is that the device collapses before final reentry begins so that the heating is higher and more destructive. It will collapse below 250 km so that it will be below any active satellites, but it must be collapsed by 150 km, which is about the start of reentry.[35] The atmospheric pressure is applied as a distributed force over the drag sail, and other disturbance forces are ignored because atmospheric pressure is the largest at these altitudes by at least an order of magnitude. Arbitrarily, the booms must not deflect more than 5% at 250 km, and must be deflected at least 50% at 150 km for this condition to be met.[35]

The nominal load case is defined as the forces on the boom due to the atmospheric pressure at 250 km applied to the 22 m x 9 m sail. The drag force due to aerodynamic pressure was found using the equations described in Section III.B.2 to be 7.8 N for the whole system, then dividing it by 4 twice for the four sails then the four mounting points of each sail. The nominal load condition is 0.49 N. A deflection analysis of a single full-length TRACv4 boom that measures 9 m long for this load case was conducted using ABAQUS finite element software. The load was not directed straight downward because the sail would most likely billow, as seen in Figure 23.

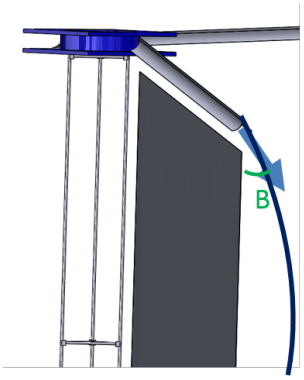

Figure 23: The billow of the sail makes the force angled slightly.

IV.E.1. Finite Element Model Definition

The TRACv4 boom is made from carbon fiber reinforce polymer (CFRP) in unidirectional tape and plain weave fabric forms that use Hexcel IM7 fibers and 977-2 resin. The material properties are can be seen

in Table 11. It is a transversely isotropic material, so only five properties are needed. The weave was modeled as several perpendicular plies of tape. The boom is basically two tape springs connected on the top ridge, so the ridge is twice as thick as the flange. The stacking sequence for the flange is [0°, ±45°, 0°], and the ridge is [0°, ±45°, 0°, 0°, ±45°, 0°].[28]

Table 11: Material properties for unidirectional Hexcel IM7/977-2 used for the TRAC booms[28]

$E_{11}(GPa)$	$E_{22}(GPa)$	ν_{12}	ν_{23}	$G_{12}(GPa)$
173	9.17	0.34	0.37	5.65

This analysis uses a detailed model of the boom as two tapes bonded together using the S4R shell element. The layers of composites were modeled as different shell element layers. The weave was modeled as 10 layers of single ply lamina alternating +45°and -45°. The combined layers that comprised the weave was thicker than one of the layers of single ply. As mentioned above, the top part has twice as many layers (24 as opposed to 12) than the flange part because that is where the two tapes overlap. The boundary conditions were applied to one end where it was fixed in all directions, and the force was applied onto the middle node at the other end with a 5° billow angle away from the negative y-direction.

IV.E.2. Results

The results of the deflection analysis can be seen in Figure 24. The maximum deflection is 0.39 m, which is 4.3% deflection compared to the total length of 9 m. This is less than the chosen 5% deflection that determines the sail is not collapsed, fulfilling the requirement. This result agree with the published values evaluated using the basic equation for deflection of a cantilever beam.[28] This confirms this boom selection.

Different billow angles were investigated, and predictably, as the billow increases the deflection in the y direction decreases. It was also investigated how the magnitude of the deflection changes when the direction of the force changes. The magnitude of the force was changed from -0.49 N to +0.49 N and the deflection had the same magnitude.

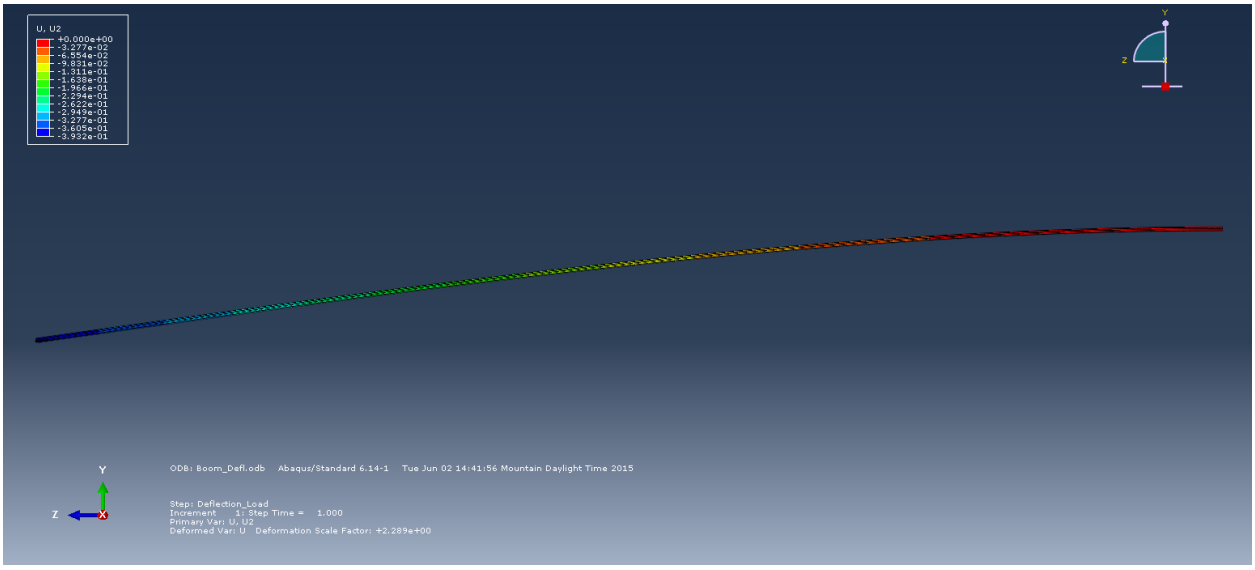

Figure 24: Deflection analysis results for TRACv4 with load of -0.49, and 5° billow.

V. Conclusion and Future Work

Orbital debris in Low Earth Orbit can no longer be ignored, and one of the most prevalent categories of objects is launch vehicle upper stages. This research investigated the different options for designing a passive

deployable drag device to attach to launch vehicles before launch in order to ensure deorbit within 25 years. It was decided that the initial design should be a drag sail with the ability to deorbit the upper stages of the three main American launch vehicles (the Falcon 9, the Delta IV, and the Atlas V) within 25 years. The baseline design is two drag sails mounted on either end of the upper stage with various angles to ensure that it is aerostable. The stability was verified for this concept using aerodynamic equations for free molecular flow and solar radiation pressure. The initial design was discussed including the requirements, component selection and mounting. Finally, a structural analysis was conducted on the booms to verify that the chosen component met the requirements of not collapsing above 250 km altitude.

The next steps of this project are to conduct a structural analysis of the main mast, and create and verify requirements for the sail mounting. It is also necessary to more fully develop the design for the boom deployer, the connections of the sails to the frame, and other conceptual aspects of the current design.

Acknowledgments

This work was funded through NASA Space Technology Research Fellowship, grant number NNX13AL54H. In addition, the authors would like to thank Mark Schoenenberger and Eric Queen of NASA Langley Research Center, Jeremy Banik of the Air Force Research Laboratory, and Dr. Massimo Ruzzene of Georgia Institute of Technology for their advice towards the completion of this work.

References

[1]Levin, E., Pearson, J., and Carroll, J., "Wholesale debris removal from LEO," *Acta Astronautica*, Vol. 73, Dec. 2011, pp. 100–108.

[2]Andrist, P., Babbitt, A., Ethier, V., Pfaff, M., Rios-Georgio, G., and Welter, T. R., "DEbris Capture and Orbital Manipulation - DECOM," *AIAA SPACE 2011 Conference & Exposition*, No. AIAA 2011-7293, Sept. 2011.

[3]Jasper, L. E., Seubert, C. R., Schaub, H., Valery, T., and Yutkin, E., "Tethered Tug for Large Low Earth Orbit Debris Removal," *AAS/AIAA Astrodynamics Specialists Conference*, Jan. 2012.

[4]Johnson, L., Whorton, M., Heaton, A., Pinson, R., Laue, G., and Adams, C., "NanoSail-D: A solar sail demonstration mission," *Acta Astronautica*, Vol. 68, March 2010, pp. 571–575.

[5]Nock, K. T., Gates, K. L., Aaron, K. M., and McRonald, A. D., "Gossamer Orbit Lowering Device (GOLD) for Safe and Efficient De-orbit," *AIAA/AAS Astrodynamics Specialist Conference*, Aug. 2010.

[6]Nock, K. T., Aaron, K. M., and McKnight, D. S., "Removing Orbital Debris with Less Risk," *Journal of Spacecraft and Rockets*, Vol. 50, No. 2, March 2013, pp. 365–379.

[7]Hoyt, R. and Forward, R., "The Terminator Tether: Autonomous Deorbit of LEO Spacecraft for Space Debris Mitigation," *38th Aerospace Science Meeting & Exhibit*, Jan. 2000.

[8]Mehrparvar, A., *CubeSat Design Specification*, The CubeSat Program, Cal Poly SLO, 13th ed., Feb 2014.

[9]Hevner, R., Holemans, W., Puig-Suari, J., and Twiggs, R., "An Advanced Standard for CubeSats," *25th Annual AIAA/USU Conference on Small Satellites*, 2011.

[10]Maly, J. R., Evert, M. E., Shepard, J. T., and Smith, C. A., "Space Access for Small Satellites on Rideshare Missions with ESPA and ESPA-Derived Payload Adapters," *IEEE Aerospace Conference*, 0.

[11]Lappas, V., Adeli, N., Visagie, L., Fernandez, J., Theodorou, T., Steyn, W., and Perren, M., "CubeSail: A low cost CubeSat based solar sail demonstration mission," *Advances in Space Research*, Vol. 48, June 2011, pp. 1890–1901.

[12]*LightSail-1 Solar Sail Design and Qualification*, May 2012.

[13]Boen, B., "Solar Sail Demonstrator," `http://www.nasa.gov/mission_pages/tdm/solarsail/solarsail_overview.html`, Accessed: Oct 2013.

[14]Knacke, T. W., *Parachute Recovery Systems Design Manual*, Para Publishing, 1st ed., 1992.

[15]"Capabilities & Services," `http://www.spacex.com/about/capabilities`, Accessed: Aug 2013.

[16]"Delta IV: The 21st Century Launch Solution," `http://www.ulalaunch.com/Products_DeltaIV.aspx`, Accessed: Aug 2014.

[17]"Atlas V: Maximum Flexibility and Reliability," `http://www.ulalaunch.com/products_atlasv.aspx`, Accessed: Aug 2014.

[18]Wall, M., "World's Largest Solar Sail to Launch in November 2014," `http://www.space.com/21556-sunjammer-solar-sail-launch-2014.html`, Accessed: Jun 2013.

[19]Jacchia, L. G., "New Static Models of the Thermosphere and Exosphere with Empirical Temperature Profiles," SAO Special Report 313, Smithsonian Institution, Cambridge, Massachusetts, May 1970.

[20]"U.S. Standard Atmosphere, 1976," Oct 1976.

[21]Suggs, R. J., "Future Solar Activity Estimates for Use in Prediction of Space Environmental Effects on Spacecraft Orbital Lifetime and Performance," Tech. rep., George C. Marshall Space Flight Center, Apr 2015, Referenced Table 3.

[22]Bird, G. A., *Molecular Gas Dynamics and the Direct Simulation of Gas Flows*, Oxford University Press, 1994.

[23]Delgado, M. R., "Radiation Pressure: Modeling the Space Environment," http://ocw.upm.es/ingenieria-aeroespacial/modeling-the-space-environment/contenidos/material-de-clase/mse07_radiationpressure.pdf, Apr 2008, European Masters in Aeronautics and Space.

[24]Fortescue, P., Stark, J., and Swinerd, G., editors, *Spacecraft Systems Engineering*, Wiley, 3rd ed., 2003.

[25]Banik, J. A., *Structural Scaling Metrics for Tensioned-Blanket Space Systems*, Ph.D. thesis, The University of New Mexico, May 2014.

[26]Murphey, T. W., *Recent Advances in Gossamer Spacecraft*, Vol. 212 of *Progress in Astronautics and Aeronautics*, chap. Booms and Trusses, AIAA, Reston, Virginia, 20006, pp. 1–43.

[27]"ATK Coilable Factsheet," www.atk.com, Accessed: May 2014 2012.

[28]Banik, J. A. and Murphey, T. W., "Performance Validation of the Triangular Rollable and Collapsible Mast," *24th Annual AIAA/USU Conference on Small Satellite*, No. SSC10-II-1, 2010.

[29]Souder, M. D. and West, M., "Solar Sail Technology for Nanosatellites," Aug. 2008.

[30]Hillebrandt, M., Meyer, S., Zander, M., and Huhne, C., "Deployment Testing of the De-Orbit Sail Flight HArdware," Jan. 2015.

[31]Murphy, D. M., McEachen, M. E., Macy, B. D., and Gaspar, J. L., "Demonstration of a 20-m Solar Sail System," April 2005.

[32]Sinn, T., Vasile, M., and Tibert, G., "Design and Development of Deployable Self-inflating Adaptive Membrane," April 2012.

[33]Vedova, F. D., Henrion, H., Leipold, M., Girot, T., Vaudemont, R., Belmonte, T., Fleury, K., and Le Couls, O., "The Solar Sail Materials (SSM) project - Status of activities," *Advances in Space Research*, Vol. 48, Aug. 2011, pp. 1922–1926.

[34]Papa, A. and Pellegrino, S., "Systematically Creased Thin-Film Membrane Structures," *Journal of Spacecraft and ...*, Vol. 45, No. 1, Jan. 2008.

[35]Harkness, P. G., *An Aerostable Drag-Sail Device for the Deorbit and Disposal of Sub-Tonne, Low Earth Orbit Spacecraft*, Ph.D. thesis, Cranfield University, Oct 2006.

Appendix A: Requirements

Table 12: The full requirements verification matrix with flow down and rationales.

ID	Mission Statement	Source	Rationale
MS	The deployable drag device shall accelerate the orbital decay rate of L/V upper stages, allowing deorbit to occur within 25 years after launch. The device shall be mounted as a secondary payload on L/V upper stages.		
ID	**Mission Objective**	**Source**	**Rationale**
MO-1	The device shall deorbit L/V upper stages for the Falcon 9, Atlas V, and Delta IV launch vehicles within 25 years from an initial orbit altitude of 850 km or less.	MS	
ID	**Mission Requirements**	**Source**	**Rationale**
M-1	The system shall de-orbit from a 850 km circular altitude (any inclination) within 25 years.	MO-1	Calculated with deployment between halfway between solar maximum and solar minimum
M-2	The system shall be capable of deorbiting the upper stages for the Falcon 9, Atlas V, and Delta IV launch vehicles.	MO-1	Most common American L/V that launch to LEO.
M-3	The system shall utilize standard secondary payload L/V interface for mounting deployable drag device found in ESPA RUG.	MS	
ID	**System Requirements**	**Source**	**Rationale**
S-1	The system shall be comprised of two separate devices mounted on either end of upper stage	M-2	Needed for aerodynamic stabilization
S-2	The combined L/V upper stage/deorbit device system shall have an area-to-mass ratio of at least 0.16 m^2/kg once the sail is deployed	M-1, S-1	Deorbit analysis shows that area-to-mass ration of 0.16 m^2/kg is necessary for deorbit within 25 years (actual estimate is 23 years). Includes two devices.
ID	**Device Requirements**	**Source**	**Rationale**
D-1	The device shall be stowed in 27U PPOD packaging	M-3, S-1	
D-2	The device shall utilize the standard PPOD interface to the launch vehicle	M-3	
D-3	The device shall be a drag sail that is passive once deployed	MO-1	Evaluated on cost, deorbit time, and risk.
D-4	The device shall have a mass of no more than 50 kg.	M-3, D-1	Max mass of 27U PPOD
D-5	The materials shall reduce outgassing according to ESPA RUG.	M-3	
D-6	The device shall not impede the breakup of the upper stage in the atmosphere.	MO-1	
ID	**Sail Subsystem Requirements**	**Source**	**Rationale**
SS-1	The sail subsystem shall have a drag area of at least 375 m^2	S-1, S-2, D-1	Calculated from,mass of Falcon 9 (most massive) upper stage, and desired area-to-mass ratio. This is half of the desired 750 m^2
SS-2	The sail subsystem shall have a stowed volume of less than 0.043 m^3, consistent with the 27U PPOD standard.	D-1	Max volume for 27U PPOD.
SS-3	The sail shall have rigid booms that support a thin sail material.	D-3	
ID	**Deployment System Requirements**	**Source**	**Rationale**
DS-1	The deployment subsystem shall only deploy the sail after all payloads have been deployed.	MO-1	Minimize impact to payloads of LV.
DS-2	The,device shall deploy within TBR minutes of final payload deployment	MO-1	The earlier it is deployed, the more effective it will be in deorbiting the upper stage
DS-3	The deployment subsystem shall keep the sail deployed for the orbit lifetime of the upper stage.	M-1, D-3	Maximize effect on deorbit of LV.
DS-4	The deployment subsystem shall not create debris while deploying the drag sail.	M-3	
DS-5	The drag sail deployed volume shall not impact any hardware associated with the launch,vehicle upper stage or secondary payloads	M-1, D-3	To prevent the sail from hitting the upper stage and preventing full deployment
ID	**Launch Vehicle Interface Requirements**	**Source**	**Rationale**
LV-1	The device shall be designed to withstand the launch environment of all launch systems planned for use.	M-2, M-3	
LV-2	The device shall be designed to the PPOD load factors.	M-3	